

Supplemental material – Erosion and weathering in carbonate regions reveals climatic and tectonic drivers of carbonate landscape evolution

Richard Ott^{1,2}, Sean F. Gallen³, David Helman^{4,5}

¹*Department of Earth Sciences, ETH Zurich, Zurich, Switzerland*

²*GFZ German Research Centre for Geosciences, Potsdam, Germany*

³*Department of Geosciences, Colorado State University, Fort Collins, US*

⁴*Department of Soil and Water Sciences, Institute of Environmental Sciences, Faculty of Agriculture, Food and Environment, Hebrew University of Jerusalem, Rehovot, Israel*

⁵*Advanced School for Environmental Studies, The Hebrew University of Jerusalem, Jerusalem, Israel*

Weathering corrections for denudation rates

Chemical weathering can bias cosmogenic nuclide-derived denudation rates. Regolith weathering can overestimate ^{36}Cl denudation rates because the soluble target mineral calcite may have a shorter regolith residence time than the bulk rock due to its high solubility. We use the methods proposed by Ott et al. (2022) to correct all alluvial denudation rates for regolith weathering. The correction requires knowledge of the regolith or bedrock composition. In the absence of direct bedrock compositional data, we use the reported bulk chemical composition of the samples as an estimate of regolith composition. We multiply the weight-percent CaO by 1.4 to estimate the calcite fraction in the regolith, take the SiO₂ weight-percent as fraction quartz, and assign the remainder as other insoluble minerals.

Additionally, we use the mean weathering rates for every area (Israel: 21 ± 3 mm/ka, Crete: 48 ± 11 mm/ka, France: 37 ± 8 mm/ka) for the corrections. On Crete, we estimate 30 cm regolith thickness within the sampled catchments from the European soil database (ESDAC) (Panagos et al., 2012). We use this thickness in conjunction with a density of 1.5 g/cm³ to derive a soil mass of 45 g/cm². The same value is found in southern France, with soil depth estimated from the maps of Chen et al. (2019). For the Soreq

catchment in Israel, Ryb et al. (2014b) report regolith thicknesses between 0 and 75 cm. We take the middle (37.5 cm) and use it with the reported regolith density of 1.4 g/cm³ to derive an average soil mass of 52.5 g/cm².

Weathering-corrected denudation rates are similar to conventional denudation rates, with a maximum difference of about 7% (Tab. S2). The sample compositions reported from southern France indicate almost pure limestone. Therefore, the bias for these rocks is very small. For five samples, the weathering correction could not be applied because the reported nuclide concentration was greater than the theoretical maximum nuclide concentration for the provided parameter combination (N_{\max} , for definition, see Ott et al., 2022). This is likely linked to uncertainties in the input parameters, such as weathering rate, regolith mass, etc. For some samples considered here, the actual catchment weathering rate is possibly lower than the mean weathering rate for the area. However, the distribution of water sampling stations does not allow deriving weathering rates close to every location sampled for cosmogenic nuclides. In general, the weathering bias in the investigated samples is low due to the low weathering rates and clean limestone composition of many samples. Because the corrections are low and uncertainty exists in some of the correction parameters, we chose to report uncorrected denudation rates in the main text.

Tab. S2: Output of weathering correction calculation for catchment-average denudation rates.

Location	Sample	Denudation rate mm/ka	err	Conventional denudation rate mm/ka	Rate difference %
Crete	Cl-617-2	87.3	7.0	93.8	6.9
Crete	Cl-617-3				rate could not be calculated because N > Nmax
Crete	Cl-617-6	108.5	5.4	111.9	3.0
Crete	Cl-617-8	159.8	22.5	166.0	3.7
Crete	Cl-617-10	141.5	9.5	146.0	3.0
Crete	Cl-617-15	142.0	13.4	144.7	1.9
Crete	WC-616-8	521.5	117.1	531.8	1.9
France	BRO1B-G	63.0	11.5	62.2	1.1
France	ORM01B-G			37.8	rate could not be calculated because N > Nmax
France	ORM02B-G	72.6	23.4	72.0	0.8
France	ORM02B-S	81.7	21.7	80.9	0.9
France	ORM03B-G	67.1	23.3	66.5	1.0
France	ORM03B-S	67.9	20.5	67.2	1.0
France	PLBS-1G	56.4	8.0	56.1	0.4
France	PLBS-1S			48.9	rate could not be calculated because N > Nmax
France	PLBS-2S	53.9	7.3	53.7	0.3
France	PLBS-3G	100.7	19.8	100.6	0.1
France	PLBS-4G	84.4	14.7	84.1	0.4
France	PLS-E1	67.4	19.3	67.2	0.3
France	PLS-E2	75.1	22.1	74.9	0.2
France	REC01B-S	98.3	28.1	97.9	0.4
France	REC02B-G	93.3	28.1	93.1	0.3
France	REC02B-S	101.8	35.0	101.4	0.4
France	ROQ01B-G	59.7	11.3	59.1	1.0
France	ROQ01B-S	70.8	12.8	70.4	0.6
France	TAP01B-G	60.0	19.6	59.5	0.9
France	TAP01B-S	74.1	21.0	73.6	0.6
France	TAP02B-G	53.5	17.4	53.0	1.0
France	TAP02B-S	56.6	17.9	56.2	0.8
France	VID01B-S	64.7	10.6	64.3	0.7
France	VID02B-S	82.5	15.3	82.1	0.5
Israel/Soreq	SQSED1			41.5	rate could not be calculated because N > Nmax
Israel/Soreq	SQSED2	60.8	1.4	63.4	4.1
Israel/Soreq	SQSED3	59.6	1.3	61.1	2.5
Israel/Soreq	SQSED4	117.3	5.3	118.7	1.1
Israel/Soreq	SQSED5	50.5	0.4	53.1	4.9

Israel/Soreq	SQSED6	58.6	1.2	59.9	2.1
Israel/Soreq	SQSED7			49.8	rate could not be calculated because N > Nmax

Tab S3: Raw and precipitation corrected water data from southern France. $[Ca^{2+}]$ and $[Mg^{2+}]$. n – number of samples, min – minimum concentration, max – maximum concentration measured.

National Code of station	Area	Lon	Lat	Ca					Mg					Cl			
				n	min	max	average	corrected	n	min	max	average	corrected	n	min	max	average
09678X0109/HY	Luberon	5.3802	43.8203	1	91.8	91.8	91.8	91.7	1	3.4	3.4	3.4	3.1	1	5.1	5.1	5.1
09685X0011/F	Luberon	5.4057	43.8285	5	77.0	85.2	80.9	80.8	5	6.5	8.7	7.6	7.3	10	3.7	4.8	4.5
09681X0069/FO	Luberon	5.4622	43.8399	2	102.4	110.0	106.2	106.0	2	3.4	3.5	3.5	2.7	2	10.1	11.4	10.8
09685X0013/F	Luberon	5.4171	43.7862	3	80.0	93.5	87.2	87.1	3	1.3	1.5	1.4	1.0	3	6.1	6.5	6.3
09685X0012/HY	Luberon	5.4226	43.7868	3	82.8	88.9	86.2	86.2	3	4.9	6.3	5.8	5.7	3	0.8	1.4	1.0
09674X0089/F	Luberon	5.3852	43.8361	3	68.0	74.0	70.7	70.4	3	2.6	3.5	3.0	2.1	3	13.9	14.9	14.3
09686X0019/F	Luberon	5.5380	43.7930	31	104.0	123.0	112.7	112.6	31	7.0	9.5	8.1	7.8	31	4.1	8.0	5.1
09676X0053/P	Luberon	5.1791	43.7531	7	55.0	120.0	103.4	102.9	7	4.4	16.1	13.5	11.8	8	10.7	31.0	25.7
09175X0016/HY	Lure	5.7888	44.1090	3	49.0	53.5	50.8	50.8	3	0.5	0.5	0.5	0.3	18	0.8	9.2	2.3
09431X0010/HY	Lure	5.8374	44.0668	5	46.0	65.5	59.4	59.3	5	0.5	1.5	1.0	0.8	24	2.3	9.2	3.3
09176X0008/TX	Lure	5.8944	44.1311	3	61.0	65.6	63.9	63.8	3	9.2	10.8	9.9	9.6	4	2.5	6.1	4.1
09431X0013/HY	Lure	5.7859	44.0506	1	87.0	87.0	87.0	86.9	1	1.9	1.9	1.9	1.6	6	3.8	5.1	4.3
09424X0015/HY	Lure	5.7059	44.0956	1	62.0	62.0	62.0	62.0	1	1.5	1.5	1.5	1.4	5	1.0	3.1	2.1
09153X1005/HY	Ventoux	5.2895	44.1881	4	56.6	65.0	61.1	61.0	4	3.7	4.1	3.8	3.6	4	2.4	3.1	2.7
09153X1004/HY	Ventoux	5.2734	44.2056	1	56.1	56.1	56.1	56.1	1	8.6	8.6	8.6	8.5	1	1.2	1.2	1.2
09154X1004/SO	Ventoux	5.3148	44.1923	3	57.2	64.0	59.5	59.5	3	1.9	2.3	2.2	2.0	3	2.1	2.5	2.3
09157X0014/HY	Ventoux	5.2233	44.1895	7	49.0	51.9	50.0	50.0	7	1.2	1.4	1.3	1.2	7	2.0	2.4	2.3
09165X1006/HY	Ventoux	5.4139	44.1248	8	73.0	85.0	77.8	77.7	8	5.1	7.5	6.2	6.0	8	2.8	3.9	3.3
09156X0074/F	Ventoux	5.2071	44.1833	8	64.5	70.4	67.0	67.0	8	1.4	2.1	1.7	1.5	9	1.9	2.4	2.2
10212X0020/HY	Sainte Victoire	5.5752	43.5188	3	60.6	139.6	89.1	88.6	3	5.5	27.6	13.2	11.8	3	17.0	27.9	21.1
10213X0051/P	Sainte Victoire	5.6411	43.5285	1	132.0	132.0	132.0	131.7	1	31.8	31.8	31.8	30.8	1	15.6	15.6	15.6
10213X0050/HY	Sainte Victoire	5.6422	43.5232	1	119.0	119.0	119.0	118.8	1	18.4	18.4	18.4	17.7	1	9.9	9.9	9.9
10213X0121/HY	Sainte Victoire	5.6013	43.5563	7	116.0	129.0	122.5	122.3	7	6.7	10.4	9.2	8.7	7	6.2	9.0	7.9
10451X0041/F	Sainte Baume	5.7711	43.3098	2	61.4	118.0	89.7	89.5	2	20.8	63.5	42.2	41.4	3	7.5	17.2	10.9
10444X0028/F	Sainte Baume	5.7559	43.3016	3	85.3	108.0	93.2	92.9	3	44.2	54.9	50.4	49.3	3	11.3	22.0	15.6
10444X0026/DA	Sainte Baume	5.7099	43.2898	9	66.8	73.4	70.0	69.8	9	27.5	31.0	28.9	28.2	9	9.7	12.0	10.6
10443X0291/HY	Sainte Baume	5.6600	43.2911	14	60.4	78.8	72.2	72.0	14	17.2	21.9	19.0	18.4	14	7.6	10.2	8.7

Tab. S4: Weathering rates calculated using estimated recharge areas from topography (Fig. S1) together with average P and AET values for the entire mountain range of the sampled spring, well or river.

Location	Country	N [°]	E [°]	[Ca ²⁺]	[Mg ²⁺]	Estimated recharge areas			Mountain range averages		
						P [mm/a]	AET [mm/a]	Dissolution rate [mm/a]	P [mm/a]	AET [mm/a]	Dissolution rate [mm/a]
Agur1	Israel	31.7207	34.9162	61	35				490	291	0.021 ± 0.005
Agur2	Israel	31.7241	34.9139	56	35				490	291	0.02 ± 0.004
Agur3	Israel	31.7074	34.9399	59	33				490	291	0.02 ± 0.004
Agur4	Israel	31.6842	34.9803	62	32				490	291	0.02 ± 0.004
Agur5	Israel	31.6796	34.9890	91	34				490	291	0.026 ± 0.006
Agur6	Israel	31.6796	35.0088	58	29				490	291	0.019 ± 0.004
Agur7	Israel	31.6789	35.0276	57	29				490	291	0.018 ± 0.004
Agur8	Israel	31.7116	35.0106	70	30				490	291	0.021 ± 0.005
EnKarem1	Israel	31.7795	35.1557	48	14				490	291	0.013 ± 0.003
EnKarem13	Israel	31.7434	35.1531	53	24				490	291	0.016 ± 0.004
EnKarem14	Israel	31.7986	35.1697	61	27				490	291	0.019 ± 0.004
EnKarem15	Israel	31.7877	35.1622	65	30				490	291	0.02 ± 0.005
EnKarem16	Israel	31.7447	35.1762	60	25				490	291	0.018 ± 0.004
EnKarem17	Israel	31.7422	35.1643	36	21				490	291	0.012 ± 0.003
EnKarem3	Israel	31.8002	35.1251	62	33				490	291	0.02 ± 0.005
EnKarem9	Israel	31.8052	35.1716	55	24				490	291	0.017 ± 0.004
Karem9+1	Israel	31.8052	35.1716	61	26				490	291	0.018 ± 0.004
Eshtaol1	Israel	31.7769	35.0103	68	37				490	291	0.022 ± 0.005
Eshtaol2a	Israel	31.7770	35.0126	66	39				490	291	0.023 ± 0.005
Eshtaol3	Israel	31.8155	35.0232	74	35				490	291	0.023 ± 0.005
Eshtaol4	Israel	31.7995	35.0120	85	38				490	291	0.026 ± 0.006
Eshtaol5	Israel	31.7772	35.0255	59	31				490	291	0.019 ± 0.004
Eshtaol6	Israel	31.8097	35.0151	85	37				490	291	0.026 ± 0.006
Eshtaol7	Israel	31.7681	35.0122	52	29				490	291	0.017 ± 0.004
Eshtaol8	Israel	31.8028	35.0189	65	29				490	291	0.02 ± 0.004
Eshtaol9	Israel	31.7892	35.0161	69	31				490	291	0.021 ± 0.005
Hartuv3	Israel	31.7605	35.0085	61	37				490	291	0.021 ± 0.005
Hartuv4	Israel	31.7505	35.0001	68	35				490	291	0.022 ± 0.005
Modieen1	Israel	31.8605	35.0330	80	40				490	291	0.026 ± 0.006
Modieen2	Israel	31.8505	35.0435	81	30				490	291	0.023 ± 0.005
Modieen3	Israel	31.8266	35.0307	66	29				490	291	0.02 ± 0.004
Modieen4	Israel	31.8402	35.0361	60	27				490	291	0.018 ± 0.004
Uriya2	Israel	31.7958	34.9491	58	36				490	291	0.02 ± 0.005
Uriya3	Israel	31.8005	34.9576	66	39				490	291	0.023 ± 0.005
Uriya4	Israel	31.8159	34.9178	76	44				490	291	0.026 ± 0.006
Uriya6	Israel	31.8016	34.9508	80	37				490	291	0.025 ± 0.006
Uriya7	Israel	31.7621	34.9643	77	37				490	291	0.024 ± 0.005
Uriya8	Israel	31.8252	34.9428	88	40				490	291	0.027 ± 0.006
Uriya9a	Israel	31.7950	34.9754	78	38				490	291	0.025 ± 0.006
09678X0109/HY	France	43.8203	5.3802	91.7	3.1	794	424	0.035 ± 0.008	773	433	0.032 ± 0.007
09685X0011/F	France	43.8285	5.4057	80.8	7.3	802	443	0.032 ± 0.007	773	433	0.03 ± 0.007
09681X0069/FO	France	43.8399	5.4622	106.0	2.7	833	337	0.054 ± 0.012	773	433	0.037 ± 0.008

09685X0013/F	France	43.7862	5.4171	87.1	1.0	806	697	0.01 ± 0.002	773	433	0.03 ± 0.007
09685X0012/HY	France	43.7868	5.4226	86.2	5.7	823	701	0.011 ± 0.003	773	433	0.032 ± 0.007
09674X0089/F	France	43.8361	5.3852	70.4	2.1	761	398	0.026 ± 0.006	773	433	0.025 ± 0.006
09686X0019/F	France	43.7930	5.5380	112.6	7.8	793	418	0.046 ± 0.01	773	433	0.041 ± 0.009
09676X0053/P	France	43.7531	5.1791	102.9	11.8	707	484	0.026 ± 0.006	725	445	0.033 ± 0.007
09175X0016/HY	France	44.1090	5.7888	50.8	0.3	1081	647	0.022 ± 0.005	923	500	0.022 ± 0.005
09431X0010/HY	France	44.0668	5.8374	59.3	0.8	962	644	0.019 ± 0.004	923	500	0.025 ± 0.006
09176X0008/TX	France	44.1311	5.8944	63.8	9.6	894	184	0.054 ± 0.012	923	500	0.032 ± 0.007
09431X0013/HY	France	44.0506	5.7859	86.9	1.6	975	613	0.032 ± 0.007	923	500	0.038 ± 0.008
09424X0015/HY	France	44.0956	5.7059	62.0	1.4	1004	586	0.027 ± 0.006	923	500	0.027 ± 0.006
09153X1005/HY	France	44.1881	5.2895	61.0	3.6	1046	399	0.042 ± 0.009	912	444	0.031 ± 0.007
09153X1004/HY	France	44.2056	5.2734	56.1	8.5	999	345	0.043 ± 0.01	912	444	0.031 ± 0.007
09154X1004/SO	France	44.1923	5.3148	59.5	2.0	942	342	0.037 ± 0.008	912	444	0.029 ± 0.006
09157X0014/HY	France	44.1895	5.2233	50.0	1.2	963	259	0.036 ± 0.008	912	444	0.024 ± 0.005
09165X1006/HY	France	44.1248	5.4139	77.7	6.0	904	493	0.035 ± 0.008	912	444	0.04 ± 0.009
09156X0074/F	France	44.1833	5.2071	67.0	1.5	891	394	0.034 ± 0.008	912	444	0.032 ± 0.007
10212X0020/HY	France	43.5188	5.5752	88.6	11.8	744	378	0.038 ± 0.008	738	366	0.038 ± 0.009
10213X0051/P	France	43.5285	5.6411	131.7	30.8	776	336	0.074 ± 0.017	738	366	0.063 ± 0.014
10213X0050/HY	France	43.5232	5.6422	118.8	17.7	735	381	0.05 ± 0.011	738	366	0.052 ± 0.012
10213X0121/HY	France	43.5563	5.6013	122.3	8.7	758	340	0.055 ± 0.012	738	366	0.049 ± 0.011
10451X0041/F	France	43.3098	5.7711	89.5	41.4	794	464	0.046 ± 0.01	773	423	0.049 ± 0.011
10444X0028/F	France	43.3016	5.7559	92.9	49.3	790	439	0.054 ± 0.012	773	423	0.053 ± 0.012
10444X0026/DA	France	43.2898	5.7099	69.8	28.2	795	516	0.029 ± 0.006	773	423	0.036 ± 0.008
10443X0291/HY	France	43.2911	5.6600	72.0	18.4	748	488	0.025 ± 0.005	773	423	0.033 ± 0.007
Kournas Lake	Greece	35.3310	24.2801	118.8	40.9	908	355	0.093 ± 0.021	900	287	0.103 ± 0.023
Vrysses	Greece	35.3764	24.2010	62.8	9.2	892	345	0.04 ± 0.009	900	287	0.045 ± 0.01
Agia Fotini	Greece	35.1396	24.5288	155.3	39.7	984	248	0.15 ± 0.033	962	397	0.115 ± 0.026
Preveli	Greece	35.1635	24.4742	86.7	24.5	940	460	0.056 ± 0.012	962	397	0.066 ± 0.015
Plakias	Greece	35.1930	24.3948	64.0	16.7	917	370	0.046 ± 0.01	962	397	0.048 ± 0.011
Lytto	Greece	35.2279	25.3620	45.5	8.4	877	350	0.029 ± 0.007	799	347	0.025 ± 0.006
Samaria	Greece	35.4371	24.1267	29.4	14.6	876	315	0.026 ± 0.006	900	287	0.029 ± 0.006
Selena	Greece	35.2905	25.5310	29.8	10.8	847	292	0.024 ± 0.005	799	347	0.019 ± 0.004
Lentas	Greece	34.9518	24.9276	51.7	30.0	847	226	0.055 ± 0.012	770	215	0.049 ± 0.011
Rouvas	Greece	35.1381	24.9606	19.7	13.0	1011	263	0.027 ± 0.006	900	287	0.022 ± 0.005
Stylos	Greece	35.4353	24.1274	23.6	12.0	876	315	0.021 ± 0.005	900	287	0.023 ± 0.005
Kiliaris River	Greece	35.4604	24.1551	39.8	5.3	785	435	0.016 ± 0.004	900	287	0.028 ± 0.006
Zaros	Greece	35.1415	24.9065	28.0	14.0	1013	257	0.034 ± 0.008	988	282	0.032 ± 0.007
Aposelemis	Greece	35.3298	25.3333	112.4	23.9	795	415	0.054 ± 0.012	799	347	0.064 ± 0.014
Kourna Lake	Greece	35.3304	24.2753	101.6	43.3	908	355	0.085 ± 0.019	900	287	0.094 ± 0.021
Kourtaliotis	Greece	35.1548	24.4730	72.3	24.9	940	460	0.049 ± 0.011	962	397	0.058 ± 0.013

Tab. S5: Pearson's r and p values for the correlation of topographic and climatic variables from catchments with alluvial samples.

Pearson's r	Denudation	Mean elevation	Mean precipitation	Mean AET	Mean runoff	Mean local relief	Mean slope
Denudation	1.000	0.470	0.684	0.357	0.387	0.652	0.503
Mean elevation	0.470	1.000	0.249	-0.335	0.631	0.338	0.024
Mean precipitation	0.684	0.249	1.000	0.577	0.509	0.773	0.797
Mean AET	0.357	-0.335	0.577	1.000	-0.409	0.372	0.648
Mean runoff	0.387	0.631	0.509	-0.409	1.000	0.473	0.207
Mean local relief	0.652	0.338	0.773	0.372	0.473	1.000	0.872
Mean slope	0.503	-0.024	0.797	0.648	0.207	0.872	1.000
p-values	Denudation	Mean elevation	Mean precipitation	Mean AET	Mean runoff	Mean local relief	Mean slope
Denudation	1.000	0.002	0.000	0.020	0.011	0.000	0.001
Mean elevation	0.002	1.000	0.112	0.030	0.000	0.029	0.879
Mean precipitation	0.000	0.112	1.000	0.000	0.001	0.000	0.000
Mean AET	0.020	0.030	0.000	1.000	0.007	0.015	0.000
Mean runoff	0.011	0.000	0.001	0.007	1.000	0.002	0.187
Mean local relief	0.000	0.029	0.000	0.015	0.002	1.000	0.000
Mean slope	0.001	0.879	0.000	0.000	0.187	0.000	1.000

Tab. S6: Pearson's r and p values for the correlation of topographic and climatic variables from catchments with weathering rates.

Pearson's r	Weathering rate	Mean slope	Mean local relief	Mean precipitation	Mean runoff
Weathering rate	1.000	0.382	0.517	0.522	0.503
Mean slope	0.382	1.000	0.944	0.671	0.687
Mean local relief	0.517	0.944	1.000	0.769	0.833
Mean precipitation	0.522	0.671	0.769	1.000	0.851
Mean runoff	0.503	0.687	0.833	0.851	1.000
p-values	Weathering rate	Mean slope	Mean local relief	Mean precipitation	Mean runoff
Weathering rate	1.000	0.000	0.000	0.000	0.000
Mean slope	0.000	1.000	0.000	0.000	0.000
Mean local relief	0.000	0.000	1.000	0.000	0.000
Mean precipitation	0.000	0.000	0.000	1.000	0.000
Mean runoff	0.000	0.000	0.000	0.000	1.000

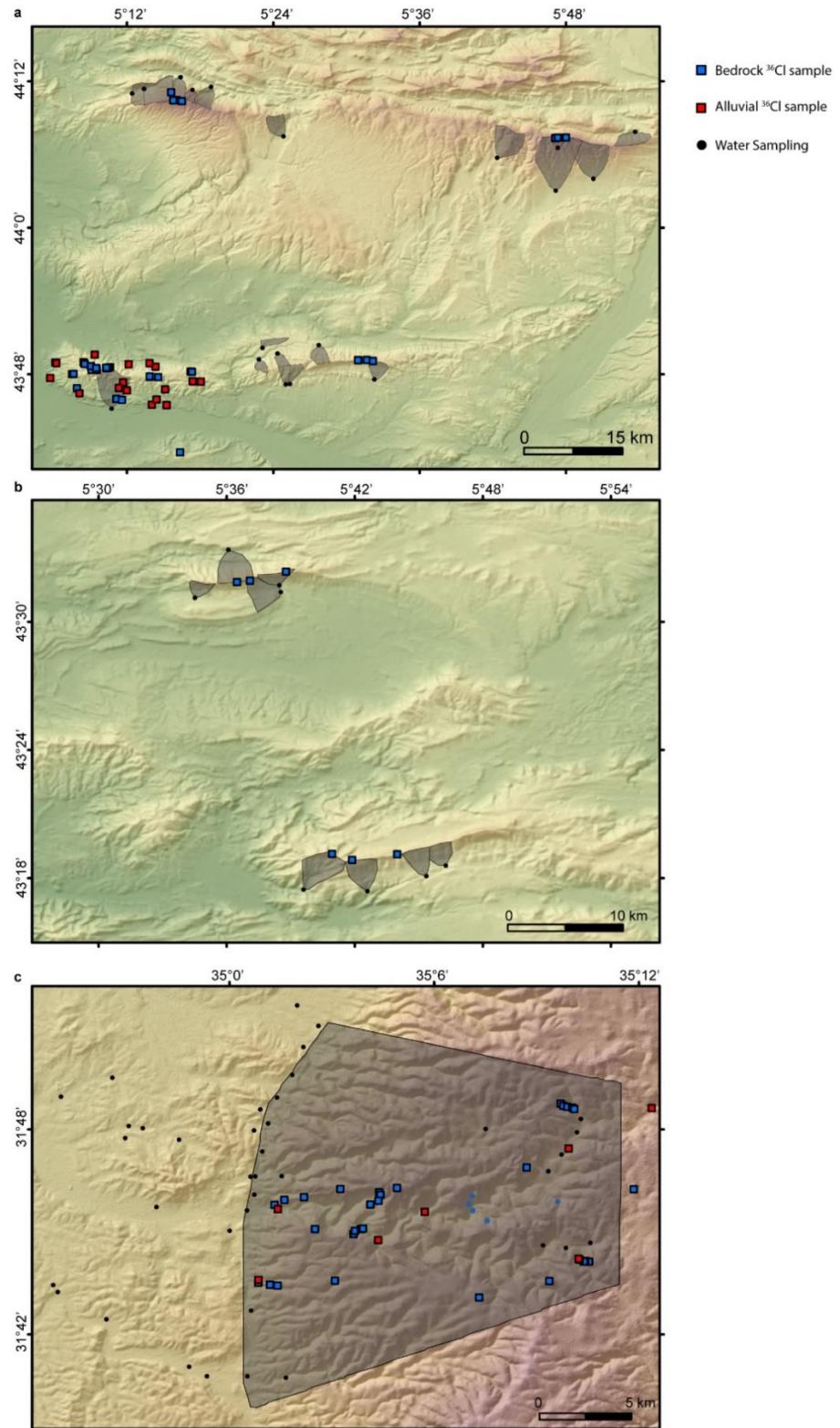


Fig. S1: Hypothetical recharge areas used to calculate the water flux required for the carbonate dissolution rate calculation for wells and springs. (a) and (b) show recharge areas for southern France, (c) for Israel, where the Western Mountain Aquifer provides the water for most wells in the coastal plain (Sheffer et al., 2010).

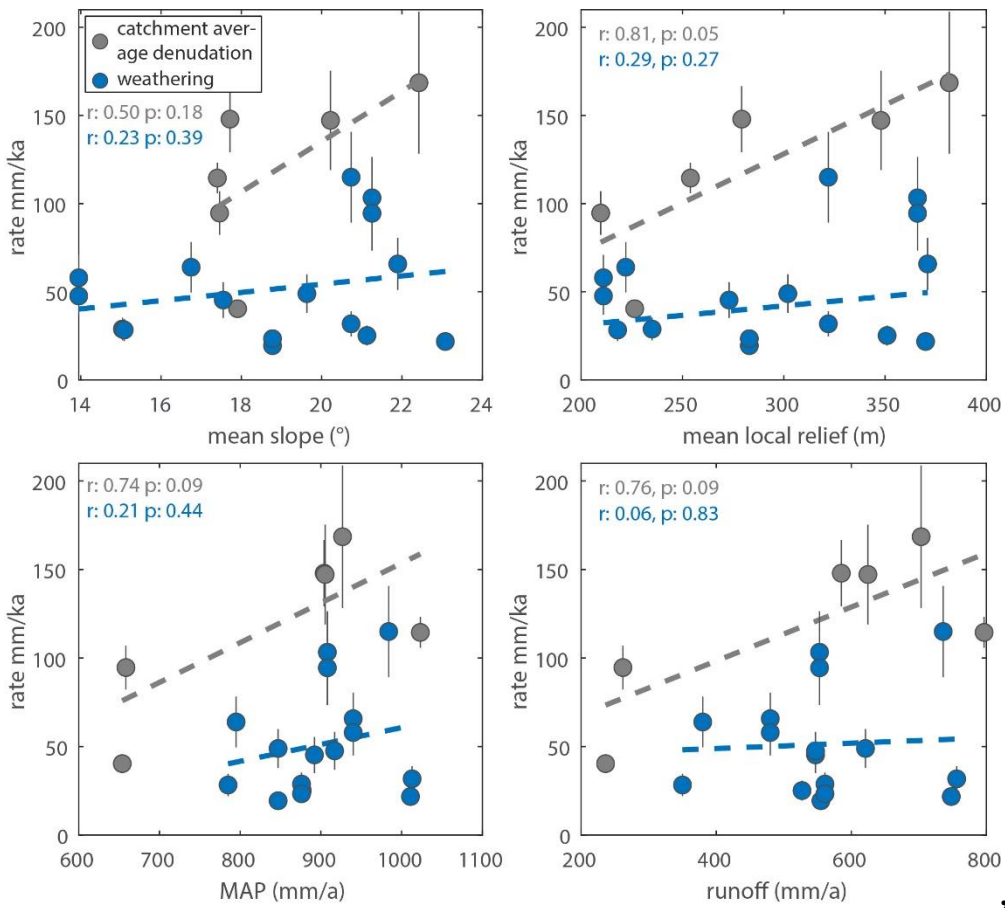


Fig S2: Correlations between catchment average ^{36}Cl denudation rates, carbonate weathering rates, and topographic and climatic metrics for samples from Crete. Values of correlation coefficient and p-values displayed for catchment-average denudation and weathering rates.

References

- Avni, S., Joseph-Hai, N., Haviv, I., Matmon, A., Benedetti, L., and Team, A., 2018, Patterns and rates of 103–105 yr denudation in carbonate terrains under subhumid to subalpine climatic gradient, Mount Hermon, Israel: *GSA Bulletin*, v. 131, p. 899–912, doi:10.1130/B31973.1.
- Ben-Asher, M., Haviv, I., Crouvi, O., Roering, J.J., and Matmon, A., 2021, The convexity of carbonate hilltops: ^{36}Cl constraints on denudation and chemical weathering rates and implications for hillslope curvature: *GSA Bulletin*, doi:10.1130/b35658.1.
- Chen, S., Mulder, V.L., Martin, M.P., Walter, C., Lacoste, M., Richer-de-Forges, A.C., Saby, N.P.A., Loiseau, T., Hu, B., and Arrouays, D., 2019, Probability mapping of soil thickness by random survival forest at a national scale: *Geoderma*, v. 344, p. 184–194, doi:10.1016/J.GEODERMA.2019.03.016.
- Godard, V., Ollivier, V., Bellier, O., Miramont, C., Shabanian, E., Fleury, J., Benedetti, L., and Guillou, V., 2016, Weathering-limited hillslope evolution in carbonate landscapes: *Earth and Planetary Science Letters*, v. 446, p. 10–20, doi:10.1016/j.epsl.2016.04.017.
- Matsushi, Y., Sasa, K., Takahashi, T., Sueki, K., Nagashima, Y., and Matsukura, Y., 2010, Denudation rates of carbonate pinnacles in Japanese karst areas: Estimates from cosmogenic ^{36}Cl in calcite: *Nuclear Instruments and Methods in Physics Research Section B: Beam Interactions with Materials and Atoms*, v. 268, p. 1205–1208, doi:10.1016/j.nimb.2009.10.134 M4 - Citavi.
- Ott, R.F., 2022, WeCode - Weathering Corrections for denudation rates V. 1.0: GFZ Data Services, doi:10.5880/GFZ.4.6.2022.001.
- Ott, R.F., Gallen, S.F., Caves-Rugenstein, J.K., Ivy-Ochs, S., Helman, D., Fassoulas, C., Vockenhuber, C., Christl, M., and Willett, S.D., 2019, Chemical versus mechanical denudation in meta-clastic and carbonate bedrock catchments on Crete, Greece, and mechanisms for steep and high carbonate topography: *Journal of Geophysical Research Earth Surface*, doi:10.1029/2019JF005142.
- Ott, R.F., Gallen, S.F., and Granger, D.E., 2022, Cosmogenic nuclide weathering biases: Corrections and potential for denudation and weathering rate measurements: *Geochronology Discussions*, doi:10.5194/gchron-2022-5.
- Panagos, P., Van Liedekerke, M., Jones, A., and Montanarella, L., 2012, European Soil Data Centre: Response to European policy support and public data requirements: *Land Use Policy*, v. 29, p. 329–338, doi:10.1016/j.landusepol.2011.07.003.
- Ryb, U., Matmon, A., Erel, Y., Haviv, I., Benedetti, L., and Hidy, A.J., 2014a, Styles and rates of long-term denudation in carbonate terrains under a Mediterranean to hyper-arid climatic gradient: *Earth and Planetary Science Letters*, v. 406, p. 142–152, doi:10.1016/j.epsl.2014.09.008.
- Ryb, U., Matmon, A., Erel, Y., Haviv, I., Katz, A., Starinsky, A., Angert, A., and Team, A., 2014b,

- Controls on denudation rates in tectonically stable Mediterranean carbonate terrain: GSA Bulletin, v. 126, p. 553–568, doi:10.1130/B30886.1.
- Sheffer, N.A., Dafny, E., Gvirtzman, H., Navon, S., Frumkin, A., and Morin, E., 2010, Hydrometeorological daily recharge assessment model (DREAM) for the Western Mountain Aquifer, Israel: Model application and effects of temporal patterns: Water Resources Research, v. 46, p. 251, doi:10.1029/2008WR007607.
- Thomas, F. et al., 2018, Limited influence of climatic gradients on the denudation of a Mediterranean carbonate landscape: Geomorphology, v. 316, p. 44–58, doi:10.1016/j.geomorph.2018.04.014.
- Thomas, F. et al., 2017, Morphological controls on the dynamics of carbonate landscapes under a mediterranean climate: Terra Nova, v. 29, p. 173–182, doi:10.1111/ter.12260.
- Xu, S., Liu, C., Freeman, S., Lang, Y., Schnabel, C., Tu, C., Wilcken, K., and Zhao, Z., 2013, In-situ cosmogenic ^{36}Cl denudation rates of carbonates in Guizhou karst area: Chinese Science Bulletin, v. 58, p. 2473–2479, doi:10.1007/s11434-013-5756-8.
- Yang, Y., Lang, Y.C., Xu, S., Liu, C.Q., Cui, L.F., Freeman, S.P.H.T., and Wilcken, K.M., 2020, Combined unsteady denudation and climatic gradient factors constrain carbonate landscape evolution: New insights from in situ cosmogenic ^{36}Cl : Quaternary Geochronology, v. 58, p. 101075, doi:10.1016/J.QUAGEO.2020.101075.